M&C 2023 - The International Conference on Mathematics and Computational Methods Applied to Nuclear Science and Engineering · Niagara Falls, Ontario, Canada · August 13 – 17, 2023

Effects of Heat and Mass Flux on Heat Transfer Characteristics in a 64-element Fuel Bundle via CFD Analysis

Huirui Han[1], Chao Zhang[1*], and Jing Jiang[2]

[1] Western University, Department of Mechanical & Materials Engineering
1151 Richmond Street, London, ON, N6A 5B9, Canada

[2] Western University, Department of Electrical & Computer Engineering
1151 Richmond Street, London, ON, N6A 5B9, Canada

hhan55@uwo.ca, czhang@eng.uwo.ca, jjiang@uwo.ca

ABSTRACT

The 64-element two-ring fuel bundle was adopted in the design of Canada's Supercritical Water-cooled Reactor (SCWR) concept. It is essential to understand the heat transfer characteristics of supercritical water in the fuel bundle so that a preliminary assessment of the safety of the nuclear reactor could be made. This paper focuses on the numerical study for investigating effects of the heat flux and mass flux on the heat transfer for the supercritical water flow in the 64-element fuel bundle. A previously validated modified turbulent model is adopted in numerical simulations. The operating conditions in simulations cover the heat flux from 600 to 880 kW/m^2, the mass flux from 860 to 4380kg/m^2·s, and the heat to mass flux ratio from 0.2 to 1.02. The results show that the bulk fluid temperature and the wall temperature generally increases with the increasing heat flux and the decreasing mass flux. The buoyancy effect based on the empirical parameter, Gr/Re$^{2.7}$ for the upward supercritical water flow in heated tubes were evaluated in this study to testify whether it still works for the rod bundle flow conditions with various heat and mass fluxes. Results show that both fluid temperature and local wall temperature distributions along the axial direction rise with the increase in the heat flux and the decrease in the mass flux. The predicted buoyancy-affected regions in the fuel bundle mainly exist around the entrance area where the fluid temperature ranges from 350 - 385˚C.

KEYWORDS: supercritical water, heat flux, mass flux, buoyancy effects

1. INTRODUCTION

The earliest studies on the heat transfer of fluids in tubes at supercritical pressures were conducted since 1960s [1-5]. Supercritical Water-cooled Reactor (SCWR) was proposed as one of the six Generation IV reactor concepts [6]. The operating pressure of the Canada SCWR concept is 25 MPa [7]. Fig. 1 shows the variations of thermophysical properties of supercritical water versus temperature at the pressure (P) of 25 MPa [8]. The pseudocritical temperature refers to the temperature where the peak specific heat exists. It can be seen thermophysical properties of the supercritical water show dramatic variations near the pseudocritical temperature. The significant decrease of the density could bring the enhanced effects of the buoyancy force and the flow acceleration on the heat transfer and the thermal conductivity drop would also impair heat transfer. Conversely, the viscosity drop brings the increase of the Reynolds number, and correspondingly boosts the flow and heat transfer. These lead to the complexity of the heat transfer

behaviors of the supercritical water in heated channels. Therefore, different heat transfer phenomena could occur at various operating conditions.

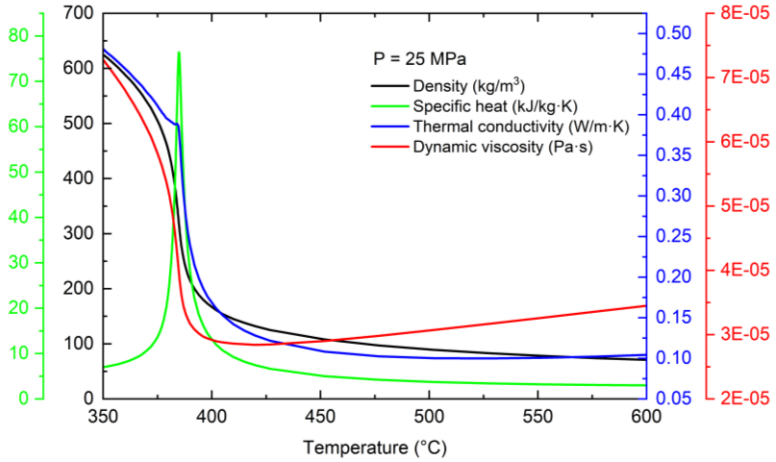

Figure 1. Variations of thermophysical properties of water at P = 25 MPa.

Many researchers investigated influences of heat flux on heat transfer behaviors in upward tubes [5,9,10], annular channels [10,11], and multiple rod bundles [12,13]under supercritical conditions. With low heat fluxes, fluid temperatures are usually below or near the pseudocritical temperature. The sharp increase of the specific heat and decrease of dynamic viscosity would enhance the heat transfer between fluid and the wall. While under high heat flux conditions, the buoyancy effects caused by dramatic density variations are more significant, which could bring the occurrence of the heat transfer deterioration. In addition, the changes of mass flux would also influence the heat transfer behaviors o supercritical water in upward heated channels. Such studies were conducted by [14,15] in tube and [13,16] in rod bundle geometries. Generally, with the increase in the mass flux, heat transfer for supercritical water in upward channels are found being improved. Efforts were made to explore effects of heat to mass flux ratio (q/G) on heat transfer characteristics. Studies indicated that the heat transfer deterioration phenomenon is more likely to happen under high heat to mass flux conditions [5,13,14,16]. The deterioration results from either buoyancy effects induced by the significant density changes along the axial direction, or acceleration effects caused by large density differences between the core and near wall regions along the radial directions. This would consequently suppress turbulent diffusion and could lead to heat transfer deterioration. Some researchers proposed relevant criteria to predict the occurrence of the heat transfer deterioration in upward supercritical water tubes [17,18]. However, the heat to mass flux ratio criteria show distinct differences under various operating conditions. Therefore, a simple heat to mass flux ratio cannot represent the onset of the heat transfer deterioration directly, other operating conditions, such as operating pressures, flow geometries should also be considered.

Existing studies on effects of the heat flux and the mass flux on heat transfer behaviors mainly focus on the supercritical water flow in tubes. However, the Canada's SCWR adopted the rod bundle concept. The flow geometry in the rod bundle is different from that in the tube, which would consequently cause differences in heat transfer characteristics, despite even with same operating conditions. In this study, numerical simulations for heat transfer behaviors of the supercritical water in an upward 64-element rod bundle were conducted by using a previously modified and validated turbulent model. The varying operating conditions cover the heat flux from 600 to 880 kW/m^2, the mass flux from 860 to 4380kg/m^2·s, and the heat to mass flux ratio from 0.2 to 1.02. An empirical parameter for predicting buoyancy-affected regions in the upward supercritical water tubes is used in this work to testify whether it still works for the supercritical water in the rod bundle with various heat and mass fluxes.

2. METHODOLOGY

2.1. Geometric Descriptions

Fig. 2a indicates the cross-section view of the physical model. The respect computational domain of the rod bundle used in this study and the definition of angles for each rod are shown in Fig. 2b. Totally 64 fuel rods are assembled in a two-ring configuration in the rod bundle. Because of the symmetry, the computational domain used in simulations is reduced to a quarter of the physical model. The supercritical water is used as the coolant and the flow direction is upward. Diameters of inner and outer rods are 9.5mm and 10mm [7]. The flow length is 5 m in the fuel bundle.

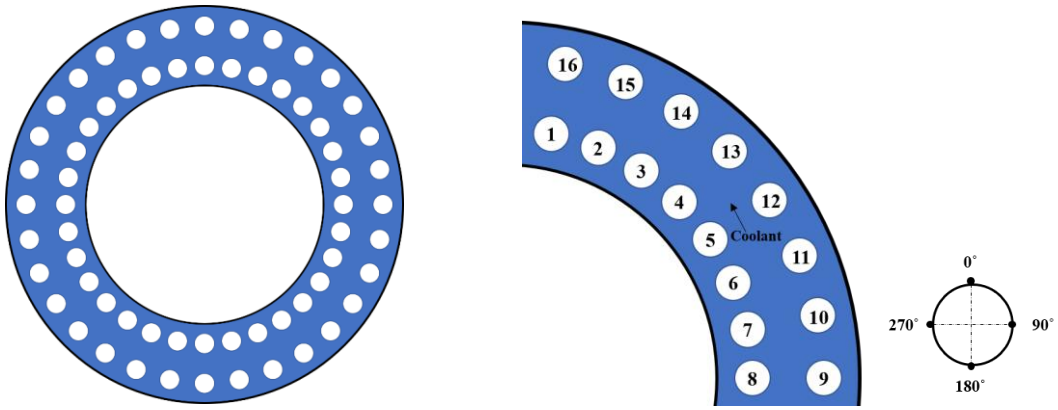

(a) Rod bundle (b) Computational domain

Figure 2. Cross-section view of the geometry.

2.2. Governing Equations and Turbulent Models

In this work, we consider fluid flow and heat transfer of supercritical water in the rod bundle domain as a steady state. The steady flow and heat transfer field are governed by conservations of mass, momentum, and energy equations, which are presented as follows [19]:

$$\frac{\partial \rho \overline{u_i}}{\partial x_i} = 0 \tag{1}$$

$$\frac{\partial (\rho \overline{u_i} \overline{u_j})}{\partial x_j} = -\frac{\partial \bar{P}}{\partial x_i} + \frac{\partial}{\partial x_j}\left(\mu \frac{\partial \overline{u_i}}{\partial x_j} - \rho \overline{u_i' u_j'}\right) + \rho g_i \tag{2}$$

$$\frac{\partial}{\partial x_i}\left(\overline{u_i}\, \rho c_p T\right) = \frac{\partial}{\partial x_i}\left[\left(\lambda + \frac{c_p \mu_t}{Pr_t}\right)\frac{\partial T}{\partial x_i}\right] \tag{3}$$

The Reynolds stress model (RSM) with a variable turbulent Prandtl number (Pr_t) [20] is used to simulate fluid flow and heat transfer behaviors in the rod bundle. It has been validated in the previous study and comparison results show it could give reasonable simulation results. Thus, it is used in numerical simulations in this study. The transport equations for the RSM are given by [19]:

$$\underbrace{\frac{\partial}{\partial x_k}\left(\rho u_k \overline{u_i' u_j'}\right)}_{C_{ij}\equiv Convection} = \underbrace{-\frac{\partial}{\partial x_k}\left[\rho\overline{u_i' u_j' u_k'} + \overline{p'\left(\delta_{kj}u_i' + \delta_{ik}u_j'\right)}\right]}_{D_{T,ij}\equiv Turbulent\ Diffusion} + \underbrace{\frac{\partial}{\partial x_k}\left[\mu\frac{\partial}{\partial x_k}\left(\overline{u_i' u_j'}\right)\right]}_{D_{L,ij}\equiv Molecular\ Diffusion} \underbrace{-\rho\left(\overline{u_i' u_k'}\frac{\partial u_j}{\partial x_k} + \overline{u_j' u_k'}\frac{\partial u_i}{\partial x_k}\right)}_{P_{ij}\equiv Stress\ Production} \underbrace{-\rho\beta\left(g_i\overline{u_j'\theta} + g_j\overline{u_i'\theta}\right)}_{G_{ij}\equiv Buoyancy\ Production} + \underbrace{\overline{p'\left(\frac{\partial u_i'}{\partial x_j} + \frac{\partial u_j'}{\partial x_i}\right)}}_{\phi_{ij}\equiv Pressure\ Strain} - \underbrace{2\mu\overline{\frac{\partial u_i'}{\partial x_k}\frac{\partial u_j'}{\partial x_k}}}_{\varepsilon_{ij}=Dissipation} \underbrace{-2\rho\Omega_k\left(\overline{u_j' u_m'}\varepsilon_{ikm} + \overline{u_i' u_m'}\varepsilon_{jkm}\right)}_{F_{ij}\equiv Production\ by\ System\ Rotation} + \underbrace{S_{user}}_{User-Defined\ Source\ Term} \tag{4}$$

In the flow domain, Pr_t is treated as a variable and calculated as:

$$Pr_t = \begin{cases} 0.4 & \mu_t/\mu < 0.2 \\ 0.3 + 0.03 * \frac{P}{P_{cr}} * Pr * (q/G) * (\mu_t/\mu) & 0.2 \le \mu_t/\mu \le 10 \\ 0.85 & \mu_t/\mu > 10 \end{cases} \tag{5}$$

Boundary conditions of simulations are presented here. For all cases, the operating pressure is 25 MPa and the inlet temperature is 350˚C. For each case, the inlet boundary condition specify the inlet mass flow rate and the inlet temperature. The outlet boundary condition employ the outflow type. The wall is considered no slip condition and the specified heat flux is assumed uniform for each fuel rod. The mesh with 13463031 cells with grid independent results are used in all simulations [13]. The near wall mesh is refined until y+ around 1 to adopt the enhanced wall treatment modeling the near wall flow region. In this study, the finite volume method is used to solve governing equations and the ANSYS FLUENT software is used for simulations. Thermophysical properties of the supercritical water at the pressure of 25 MPa from the NIST standard database [21] were incorporated into the FLUENT solver by using the piecewise-linear function of the temperature. The SIMPLEC scheme is used for the pressure-velocity coupling, and the QUICK method is used for the space discretization. The convergence criteria of all residuals are set as 10^{-6}. Operating conditions of all cases used in this work are listed in Table I.

Table I.: Operation conditions for cases in this study.

Case #	Heat flux (kW/m^2)	Mass Flux (kg/m^2·s)	Heat to mass flux ratio
1	600	861.2	0.70
2	650	861.2	0.75
3	700	861.2	0.81
4	750	861.2	0.87
5	800	861.2	0.93
6	850	861.2	0.99
7	879.9	861.2	1.02
8	879.9	1095.8	0.80
9	879.9	1315.1	0.67
10	879.9	1534.4	0.57
11	879.9	1753.5	0.50
12	879.9	2191.6	0.40
13	879.9	2630.2	0.33

14	879.9	3068.2	0.29
15	879.9	3444.7	0.26
16	879.9	3944.9	0.22
17	879.9	4383.6	0.20

3. RESULTS

3.1. Effects of Heat Fluxes

The local wall temperature distributions (T_w) at the 0˚ of Rod # 4 along the axial direction are selected to compare the local heat transfer characteristics in the fuel bundle under different operating conditions. In addition, the corresponding distributions of the bulk fluid temperature (T_b), which is defined as the mass-weighted average supercritical water temperature at the cross section along the axial direction are also compared. The buoyancy effect is one of reasons which would lead to the possible occurrence of the heat transfer deterioration. The parameter, $Gr/Re^{2.7}$, which is used for predicting the onset of the buoyancy effect for upward supercritical water circular tubes, is adopted in this study to evaluate buoyancy effects on heat transfer in the rod bundles[13], [22]. The region could be considered buoyancy-affected area if $Gr/Re^{2.7} > 10^{-5}$. Fig. 3 presents temperature distributions and evaluation results of buoyancy effects under different heat flux conditions. With the increase in the heat flux, distributions of the bulk fluid temperature and the wall temperature along the axial direction show a growth trend accordingly. In addition, although the bulk fluid temperature rises more rapidly near the exit, the wall temperature near the exit go up relatively lower. The fluid region in the rod bundle is categorized into buoyancy-affected and buoyancy-free regions by the prediction of $Gr/Re^{2.7}$. From Fig. 3c, it can be seen that buoyancy-affected regions mainly exist at the entrance region at z < 1 - 1.3 m. Such zones are reduced with the increase of the heat flux. The fluid temperature ranges from 350 to 385˚C where the density of the supercritical water do drop significantly in fact at the same zones, as shown in Fig.1. This implies that it is reasonable to use $Gr/Re^{2.7}$ to evaluate buoyancy effects in the rod bundle.

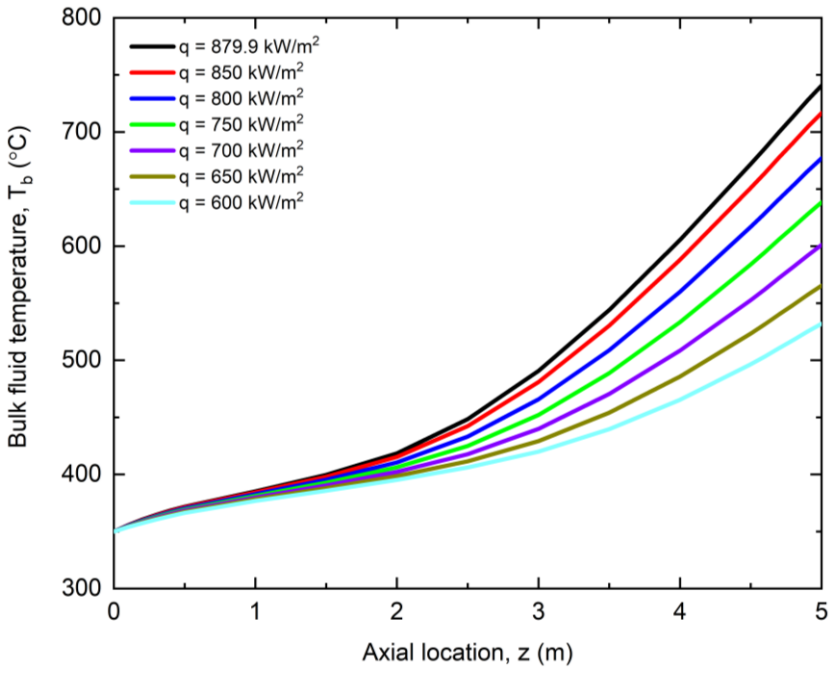

(a) Bulk fluid temperature

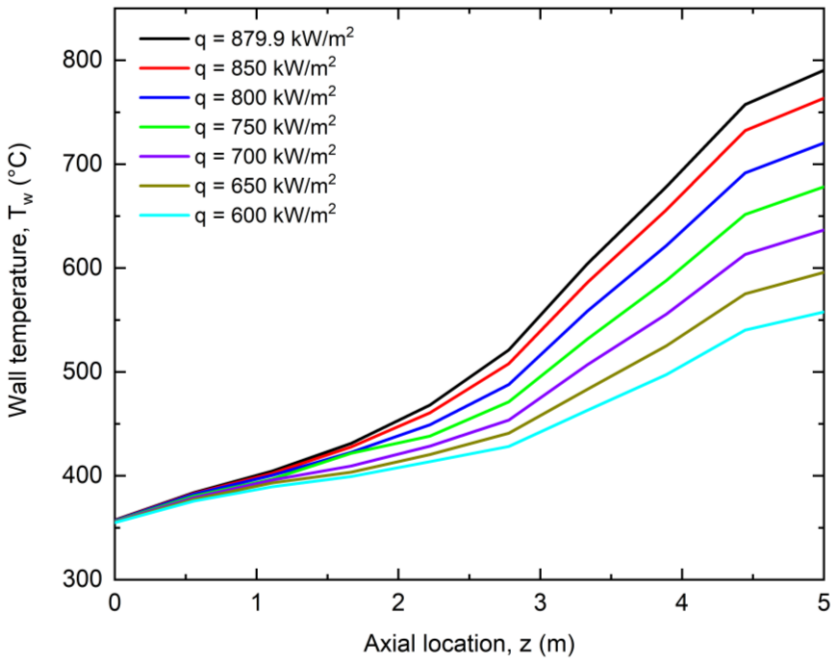

(b) Wall temperature

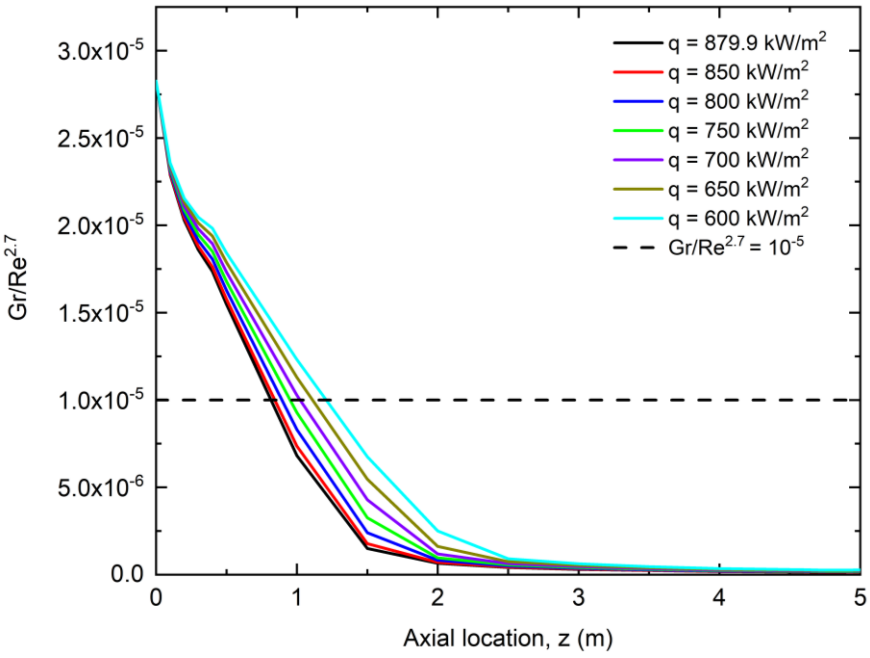

(c) $Gr/Re^{2.7}$

Figure 3. Temperature distributions and evaluation of buoyancy effects with various heat fluxes.

3.2. Effects of Mass Fluxes

Fig. 4 show temperature distributions along the axial direction and the prediction of buoyancy effects by $Gr/Re^{2.7}$ in the fuel bundle under various mass flux conditions. The heat flux is kept as 879.9 kW/m^2 while the mass flux value increase from 861.2 k to 4383.6 $kg/m^2 \cdot s$. Bulk fluid temperature and wall temperature

distributions along the axial direction generally decrease with a rise in the mass flux. When the mass flux is more than 3000 kg/m^2·s, both fluid and wall temperatures show relatively moderate and similar variations. According to prediction results by Gr/Re$^{2.7}$ in Fig. 4c, buoyancy-affected zones exist in the near entrance regions only when the mass flux is below 1095.8 kg/m^2·s.

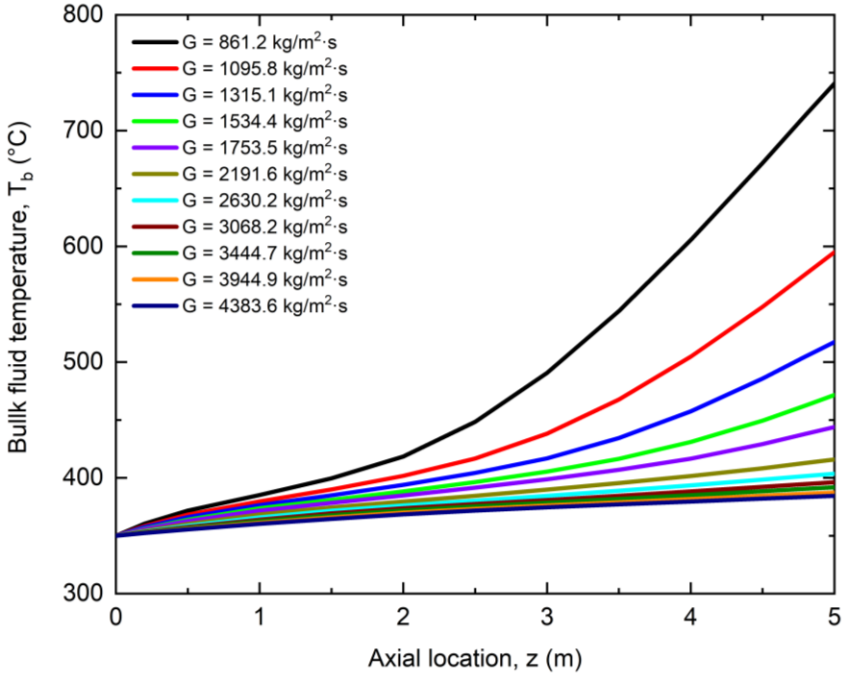

(a) Bulk fluid temperature

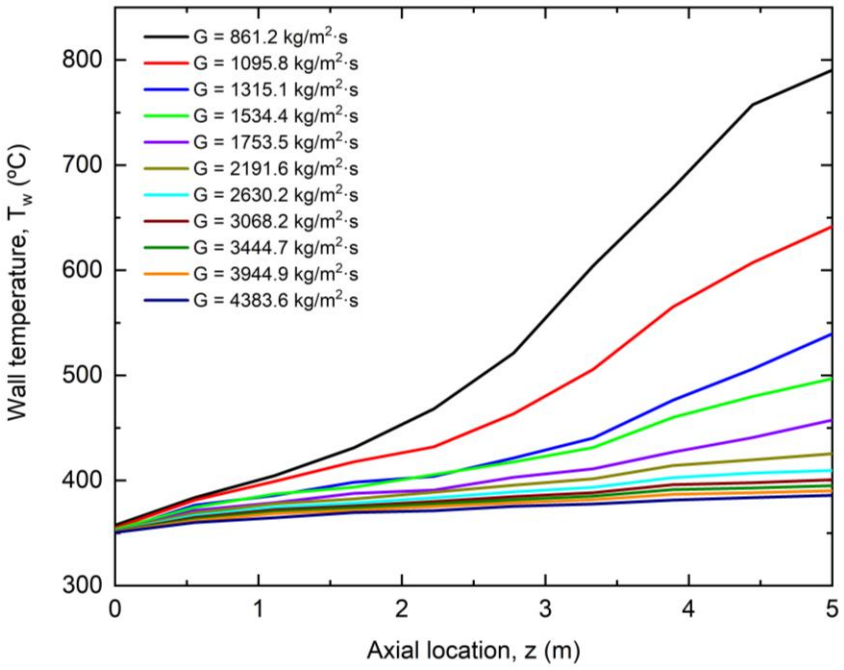

(b) Wall temperature

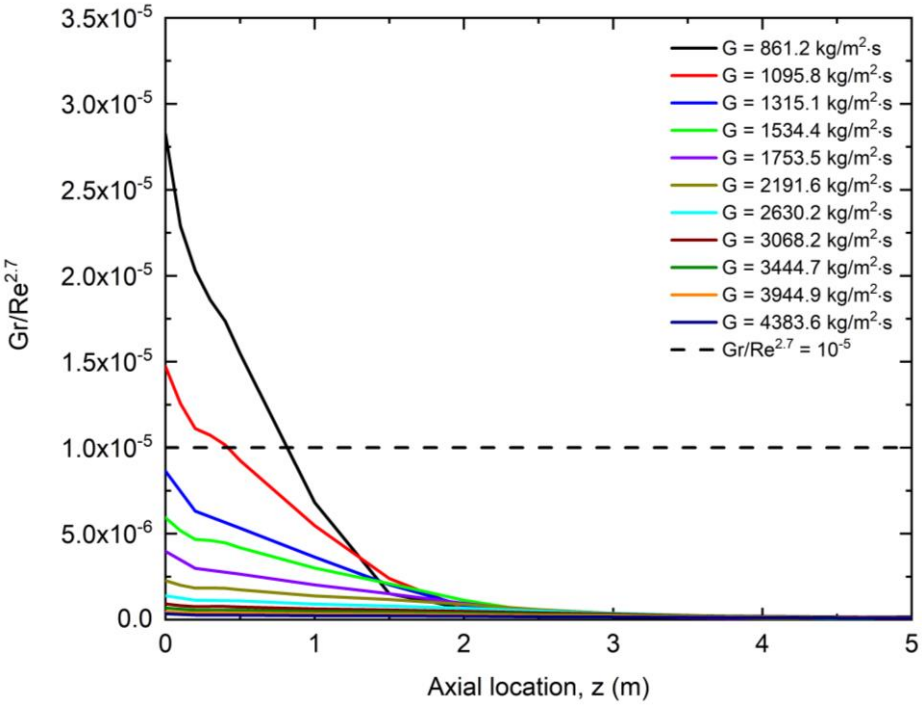

(c) $Gr/Re^{2.7}$

Figure 4. Temperature distributions and evaluation of buoyancy effects with various mass fluxes.

4. CONCLUSIONS

In this work, numerical simulations to investigate heat transfer characteristics of the supercritical water with different heat and mass flux conditions in the 64-element fuel bundle are performed. Based on the numerical results, both the bulk fluid temperature and the wall temperature generally increase with the increment in the heat flux and the drop of the mass flux. The parameter $Gr/Re^{2.7}$ used in the literature for predicting buoyance effects in the upward supercritical water tube flow is proven reasonable to be applicable in the rod bundle flow conditions. It was found that buoyancy-affected zones tend to get larger with the decrease in the heat flux and the mass flux. However, the occurrence of buoyancy effect doesn't surely mean the inevitable occurrence of the heat transfer deterioration. Other thermophysical properties of the supercritical water also vary with the operating conditions and the flow regime in the rod bundle is not the same as that in the tube, which would influence the fluid flow and heat transfer characteristics. Detailed investigations will be further explored in our future studies.

ACKNOWLEDGMENTS

The authors would like to thank the Natural Sciences and Engineering Research Council of Canada (NSERC) for financially support the work reported in this paper.

REFERENCES

1. M. Shitsman, "Impairment of the heat transmission at supercritical pressures," *High Temp.*, **1**, pp. 237-244(1963).

2. H. S. Swenson, J. R. Carver, C. R. Kakaraka, "Heat transfer to supercritical water in smooth-bore tubes," *J. Heat Transfer*, **87**(4), pp. 477-483 (1965).
3. B. Shiralkar and P. Griffith, "Deterioration in heat transfer to fluids at supercritical pressure and high heat fluxes," *J. Heat Transfer*, **91**(1), pp. 27-36 (1969).
4. A. P. Ornatskij, L. F. Glushchenko, and S. I. Kalachev, "Heat transfer with rising and falling flows of water in tubes of small diameter at supercritical pressures," *Thermal Engineering*, **18**(5), pp. 137-141 (1971).
5. K. Yamagata, K. Nishikawa, S. Hasegawa, T. Fujii, and S. Yoshida, "Forced convective heat transfer to supercritical water flowing in tubes," *Int. J. Heat Mass Transf.*, **15**(12), pp. 2575-2593 (1972).
6. US DOE, NERAC, and GIF, "A Technology Roadmap for Generation IV Nuclear Energy Systems," 2002.
7. M. Yetisir, H. Hamilton, R. Xu, M. Gaudet, D. Rhodes, M. King, K. Andrew, B. Benson, "Fuel Assembly Concept of the Canadian Supercritical Water-Cooled Reactor," *J. Nucl. Eng. Radiat. Sci.*, **4** (1), pp. 1-7 (2018).
8. I. Pioro and S. Mokry, *"Thermophysical Properties at Critical and Supercritical Pressures," in Heat Transfer - Theoretical Analysis, Experimental Investigations and Industrial Systems*, InTech, pp. 573-592 (2011).
9. J. Wang, H. Li, S. Yu, and T. Chen, "Investigation on the characteristics and mechanisms of unusual heat transfer of supercritical pressure water in vertically upward tubes," *Int. J. Heat Mass Transf.*, **54**(9–10), pp. 1950-1958, Apr. 2011.
10. L. Liu, Z. Xiao, X. Yan, X. Zeng, and Y. Huang, "Heat transfer deterioration to supercritical water in circular tube and annular channel," *Nucl. Eng. Des.*, **255**, pp. 97-104 (2013).
11. W. Gang, Q. Bi, Z. Yang, H. Wang, X. Zhu, H. Hao, L. K. H. Leung, "Experimental investigation of heat transfer for supercritical pressure water flowing in vertical annular channels," *Nucl. Eng. Des.*, **241**(9), pp. 4045-4054 (2011).
12. H. Wang, Q. Bi, L. Wang, H. Lv, and L. K. H. Leung, "Experimental investigation of heat transfer from a 2 × 2 rod bundle to supercritical pressure water," *Nucl. Eng. Des.*, **275**, pp. 205-218, Aug. 2014.
13. H. Han and C. Zhang, "Numerical investigations of the effect of operation conditions on the heat transfer of the supercritical water in the Canadian SCWR fuel bundle," *J. Supercrit. Fluids*, **191**, p. 105760, Dec. 2022.
14. X. Hao, P. Xu, H. Suo, and L. Guo, "Numerical investigation of flow and heat transfer of supercritical water in the water-cooled wall tube," *Int. J. Heat Mass Transf.*, **148**, p. 119084 (2020).
15. W. Zhang, H. Li, Q. Zhang, X. Lei, and Q. Zhang, "Experimental investigation on heat transfer deterioration of supercritical pressure water in vertically-upward internally-ribbed tubes," *Int. J. Heat Mass Transf.*, **120**, pp. 930-943, May. 2018.
16. M. Zhao and H. Y. Gu, "Experimental and numerical investigation on heat transfer of supercritical water flowing upward in 2 × 2 rod bundles," *Nucl. Eng. Des.*, **370**, no. October, p. 110903, Dec. 2020.
17. V. A. Grabezhnaya and P. L. Kirillov, "Heat transfer under supercritical pressures and heat transfer deterioration boundaries," *Therm. Eng.*, **53**(4), pp. 296-301, Apr. 2006.
18. M. T. Kao, M. Lee, Y. M. Ferng, and C. C. Chieng, "Heat transfer deterioration in a supercritical water channel," *Nucl. Eng. Des*., **240**(10), pp. 3321-3328 (2010).
19. ANSYS, "Ansys Fluent Theory Guide," (2013).
20. H. Han and C. Zhang, "A Modified Turbulent Model for the Supercritical Water Flows in the Vertical Upward Channels," *J. Supercrit. Fluids.*, **187**, p. 105632 , Aug. 2022.
21. Lemmon E., Huber M., MeLinden M., 2013. NIST reference fluid thermodynamic and transport properties-RFFPROP, version 9.1. National Institute of Standard Technology. 2013.
22. S. Mao, T. Zhou, C. Xue, and D. Wei, "Performance analysis of heat transfer for supercritical water cooled in various inclined tubes," *Nucl. Eng. Des.*, **404**, no. October 2022, p. 112184, 2023.